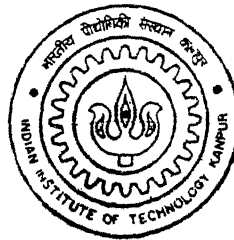


# Downlink Performance Evaluation of DS-CDMA system over Nakagami-m Fading Channel

by  
Prabhat Patel



TH  
EE/2001/M  
P 272 d

DEPARTMENT OF ELECTRICAL ENGINEERING  
INDIAN INSTITUTE OF TECHNOLOGY, KANPUR  
March, 2001

# Downlink Performance Evaluation of DS-CDMA system over Nakagami-m Fading Channel

*A Thesis Submitted  
in Partial Fulfillment of the Requirements  
for the Degree of  
Master of Technology*

by  
**Prabhat Patel**



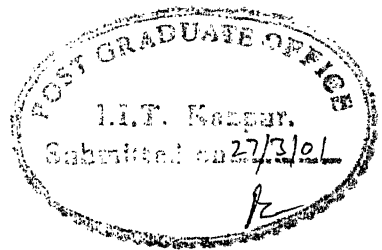
*to the*  
**DEPARTMENT OF ELECTRICAL ENGINEERING  
INDIAN INSTITUTE OF TECHNOLOGY, KANPUR**

**March, 2001**

केन्द्रीय प्रतिकालय  
भा० प्रौ० वि० कानपुर  
अवधि-क्र० A.133905



A133905



## Certificate

This is to certify that the work contained in the thesis entitled "*Downlink Performance Evaluation of DS-CDMA system over Nakagami-m Fading Channel*", by *Prabhat Patel*, has been carried out under my supervision and that this work has not been submitted elsewhere for a degree.

March, 2001

A handwritten signature in cursive script, which appears to read "Chaturvedi".

---

(Dr. A. K. Chaturvedi)

Assistant Professor,

Department of Electrical Engineering,

Indian Institute of Technology,

Kanpur.

I take this opportunity to express my sincere and deep sense of gratitude towards my thesis supervisor Dr. A. K. Chaturvedi for his constant encouragement, co-operation and invaluable suggestions during this thesis work.

Words cannot express my feelings toward my parents, brother, bhabhiji and sisters as their blessings and love has placed me where I am today. My sincere thanks to my friends and colleagues Sahuji, Vishwanathji, Satyendra, Pradeep, Anil, Shahrukh for providing me a very healthy company during my stay at I. I. T Kanpur.

I must thank my wife, Ashima, for providing me constant moral support, encouragement and for exhibiting extra ordinary patience throughout this thesis work.

This thesis is dedicated to my son Prakhar.

**Prabhat Patel**

## Abstract

IS-95 is the only CDMA based second generation standard for cellular communication. Its performance has been evaluated over Rayleigh fading channel by many investigators. However, Nakagami-m channel model is considered to be more appropriate for frequency selective fading channels. It includes the Rayleigh fading channel and one sided Gaussian as special cases. In this thesis the BER performance of forward link (base station to mobile station) of IS-95 standard has been evaluated. The multipath channel model assumes independent paths with Nakagami-m fading statistics. RAKE receiver has been used to evaluate the performance under various multipath fading conditions. The results indicate that for  $m < 1$ , the performance is worse when compared to the performance with Rayleigh fading channel model, whereas it gets better for  $m > 1$ . Also, more than 20 users can access the channel (assuming 64 chips Walsh code) simultaneously and can achieve uncoded BER of 0.01 with an average SNR of around 10 dB.

# Contents

<b>1</b>	<b>Introduction</b>	<b>1</b>
1.1	Spread Spectrum Systems . . . . .	1
1.1.1	DS-CDMA . . . . .	2
1.2	Channel Considerations . . . . .	4
1.3	Motivation for the Present Work . . . . .	4
1.4	Organization of the Thesis . . . . .	5
<b>2</b>	<b>Review of Fading Channels</b>	<b>6</b>
2.1	Features of fading channels . . . . .	6
2.1.1	Slow and Fast fading . . . . .	7
2.1.2	Frequency-Flat and Frequency-Selective fading . . . . .	7
2.2	Modeling of fading channels . . . . .	8
2.2.1	Nakagami-m model . . . . .	11
2.2.2	Characteristics of Nakagami-m distribution . . . . .	12
2.3	Diversity Techniques . . . . .	13
2.3.1	Diversity combining techniques . . . . .	14
<b>3</b>	<b>Downlink Analysis</b>	<b>17</b>
3.1	Probability of Error for Nakagami-m channel . . . . .	20
<b>4</b>	<b>Simulation Methodology</b>	<b>22</b>
4.1	Transmitter . . . . .	22
4.2	Channel . . . . .	25
4.2.1	simulation steps for $m \geq 1$ . . . . .	25

4.2.2	simulation steps for $m < 1$ . . . . .	27
4.3	Receiver . . . . .	29
<b>5</b>	<b>Results and Conclusion</b>	<b>31</b>
5.1	Scope for Future work . . . . .	36
	<b>References</b>	<b>37</b>



# List of Figures

1.1	Block diagram of DS-CDMA transmitter . . . . .	3
1.2	Block diagram of DS-CDMA receiver . . . . .	3
2.1	Multipath propagation model[3] . . . . .	9
2.2	The distribution of delays[11] . . . . .	10
2.3	Nakagami PDF for $\Omega = 1$ and various values of the fading parameter $m$ . . . . .	11
2.4	Block diagram for EGC and selection combining techniques [11] . . . . .	15
2.5	Block diagram for MRC technique [11] . . . . .	15
3.1	Multiuser modulator and multipath channel[3] . . . . .	18
3.2	Rake demodulator for multipath propagation[3] . . . . .	19
4.1	Block diagram of transmitter for single-user [11] . . . . .	23
4.2	SSRG configuration for generation of (a) In-phase PN sequence (b) Quadrature PN sequence [11] . . . . .	24
4.3	FIR Filter specifications [11] . . . . .	24
4.4	Impulse response of FIR filter [11] . . . . .	26
4.5	Simulation model for Nakagami- $m$ fading channel . . . . .	28
5.1	Autocorrelation function of I-phase PN code . . . . .	32
5.2	Autocorrelation function PN code of length 15. . . . .	32
5.3	Simulation results for $m= 0.5, 0.7$ and $1.0$ . . . . .	33
5.4	Simulation results for $m= 1, 3, 5$ and $9$ . . . . .	34
5.5	Results for $m=3$ with varying number of users . . . . .	34
5.6	Curves for Chernoff bound and simulation result for $m=1$ . . . . .	35
5.7	Curves for Upper bound, Chernoff bound and simulation result for $m=3$ . . . . .	35

# List of Tables

4.1	Coefficients of FIR filter [11] . . . . .	26
-----	---	----

# Chapter 1

## Introduction

In recent years, there has been considerable interest in the application of Code Division Multiple Access (CDMA) techniques to multiple access communications. CDMA can potentially accommodate more users than either Time Division Multiple Access (TDMA) or Frequency Division Multiple Access (FDMA), because as additional users are activated, the system performance as seen by any single user is degraded only slightly. Thus, as long as the increase in Bit Error Rate (BER) is tolerable, the already established links remain operational. Another advantage of CDMA is that there are no requirements for precise time or frequency coordination among users as in TDMA or FDMA. Furthermore, CDMA offers the usual benefits associated with spread spectrum systems such as interference rejection/suppression and multipath mitigation.

### 1.1 Spread Spectrum Systems

The spread spectrum system is a wideband system which expands the system bandwidth several times the message bandwidth. It has been defined as [1] “Spread spectrum is a means of transmission in which the signal occupies a bandwidth in excess of the minimum necessary to send the information; the band spread is accomplished by means of a code which is independent of the data, and a synchronized reception with the code at the receiver is used for De-spreading and subsequent data recovery.” The applications of spread spectrum technique are many fold[2, 1]:

1. Interference suppression
2. Energy density reduction
3. Ranging or time delay measurement
4. Anti-jamming
5. Multiple user random access communications with selective addressing capability
6. Anti-interference
7. Low probability of intercept
8. Accurate universal timing

A significant feature of a spread spectrum system is its *Immunity to multipath reception*. In a wireless system a signal transmitted may reach the receiver via different paths ( being reflected and diffracted by various terrain configurations) apart from a direct path. Also there are situations when no direct path is available. This results in a distorted received signal, which is also known as self jamming. But a spread spectrum system is resistant to such situations and diversity techniques can be employed to separate different component path signals which can be processed further to demodulate received signal. Because of the possibility of random access communication, the spread spectrum communication system is also called spread spectrum multiple access (SSMA) communication. The SSMA system is divided into Direct sequence CDMA (DS-CDMA), Frequency Hopping CDMA (FH-CDMA) and hybrid CDMA. DS-CDMA is most important amongst all three and hence it is only being considered in this thesis.

### 1.1.1.1 DS-CDMA

DS spread spectrum signals are generated by linearly modulating the data stream with a wideband signal. This wideband signal is known as signature sequence. This sequence is assigned to a user and is unique to each user. The block diagram of a DS-CDMA system is shown in Fig. 1.1. In a mobile communication environment, the important characteristics of the DS-CDMA are universal frequency reuse, efficient power control,

soft hand off of the mobile, and enhancement of capacity using sectorized antenna etc. [3]. Referring to Fig. 1.1, the data source is modulated by the PN sequence of the

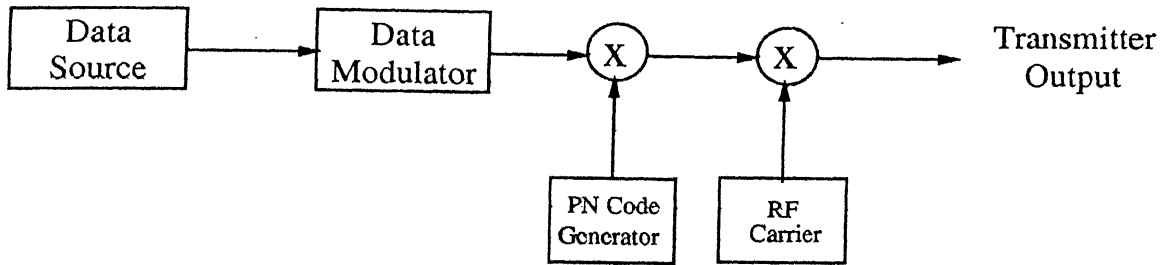


Figure 1.1: Block diagram of DS-CDMA transmitter

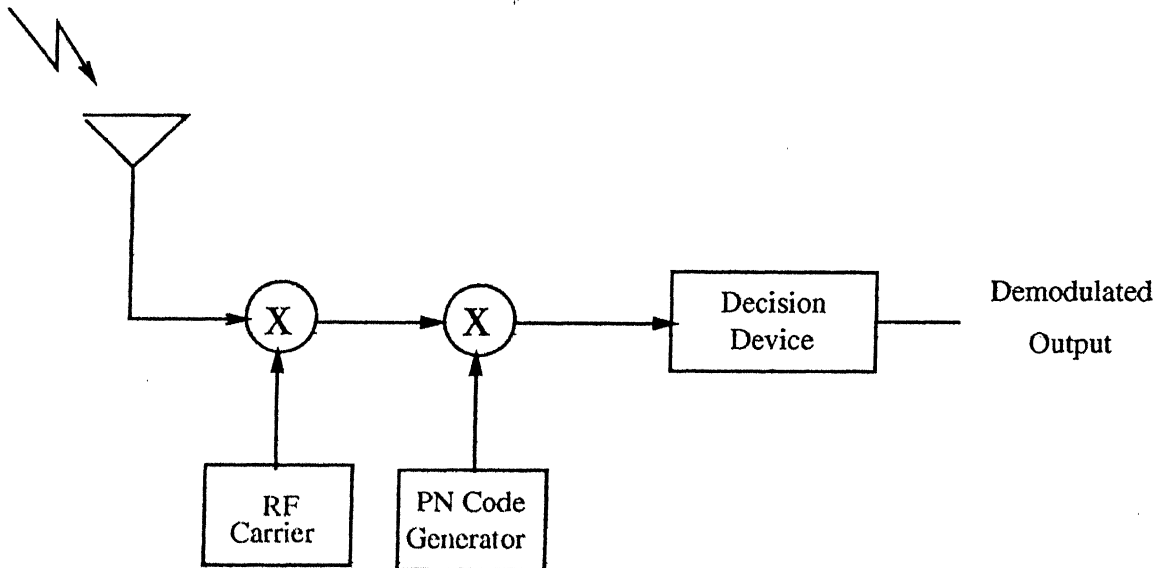


Figure 1.2: Block diagram of DS-CDMA receiver

user followed by carrier signal. The PN sequence is a stream of 1's and 0's whose rate is manifold higher than the data rate. Individual bit of a PN sequence is called a *chip*. The ratio of the PN sequence rate to the data rate is known as processing gain of the system. The receiver structure for the DS-CDMA system is shown in Fig. 1.2. The received signal from the channel output is carrier demodulated and then passed through a correlator which correlates the carrier demodulated received signal with the locally generated PN code of the user. Here it is assumed that the locally generated PN sequence generator is in synchronism with that of the transmitter. The correlator output is fed to a decision device which makes some processing and detects the bits.

## 1.2 Channel Considerations

A prerequisite for the performance analysis of mobile communication system is a model for channel behavior i.e. fading statistics. With an accurate channel model, it becomes feasible to compare various systems. Typical wave phenomena like scattering, diffraction, and absorption by physical structures in the environment leads to a diffusion of a transmitted wave into a continuum of partial waves with different amplitudes and phases [7]. As a result, a transmitted signal, modulating a carrier wave is attenuated and distorted. These effects depend on the geometrical and electromagnetic properties of the physical transmission environment. Real environments show a broad variation of the physical properties, leading to varying channel behavior. Typically, the scattering structures are irregularly distributed. The scattered partial waves interfere spatially and build up an irregularly distributed interference pattern. Such circumstances have led to a large number of extensive experiments and numerous theoretical investigations to be performed on the intensity distribution of fading under various conditions. As a result diverse forms of the distributions have been presented. Amongst them, following three may be regarded, in view of practical uses, as the representatives [6].

- Rayleigh Distribution

The applicability of this distribution to fading in many practical channels has been confirmed by many investigators.

- Log-normal Distribution

Log-normal law is often followed over long periods over which the short-term fading is nonstationary.

- Nakagami-m Distribution

This distribution degenerates to Rayleigh distribution for  $m = 1$ .

## 1.3 Motivation for the Present Work

The BER performance of each user in a CDMA system is affected by fading statistics of the received signal. A series of propagation experiments conducted in typical ur-

ban/suburban areas have revealed the multipath nature of the mobile radio channel resulting from reflection, refraction, and scattering by buildings and other obstructions in the vicinity of the mobile [5, 14]. Multipath propagation can be resolved at the receiver of a DS-CDMA system since it uses a bandwidth much larger than the coherence bandwidth of the channel. The problem of obtaining the distribution of the signal strength of each path coincides with the random phaser interference problem. Nakagami-m distribution provides a more general solution for such a problem as compared to Rayleigh and Rice distributions, which are only special case solutions [6, 7]. It has been shown that such multipath scenario in urban/suburban areas are better modeled by Nakagami-m distribution [4, 5, 6]. As a brief digression, the Nakagami-m distribution is also of great interest to ionospheric physicists because amplitude fading due to ionospheric scintillation has been found to follow an m-distribution [9].

It has been established that Nakagami-m distribution model is best fit for mobile communication system channel model. Though lot of work has been carried out to evaluate the performance of DS-CDMA systems over Rayleigh fading channel, the use of Nakagami-m channel model would be more appropriate. It would be of interest to analyse how IS-95, which is leading 2<sup>nd</sup> generation standard for mobile communication, performs when incorporated through Nakagami-m channel. In this work, a channel model incorporating Nakagami multipath fading is developed and the BER performance of IS-95 standard using coherent demodulation has been evaluated. For simulation purpose only the forward link of IS-95 standard [11] has been used incorporating the RAKE receiver [3] using Maximal Ratio Combining (MRC) technique [8].

## 1.4 Organization of the Thesis

Chapter 2 contains the details of the multipath channel characteristics and various methods to alleviate the effect of the interference resulting due to multipath. Chapter 3 gives detailed analysis of forward link of DS-CDMA system. In chapter 4 the implementation steps have been described in detail. Chapter 5 presents the results, conclusion and the scope for future work.

# Chapter 2

## Review of Fading Channels

Any communication system has transmitter, receiver and in between the two is the channel. For mobile communication system the transmitter and the receiver may be mobile. When the data or voice is transmitted from the base station (BS) the transmitter is fixed whereas the receiver (mobile station MS) is movable. The link from the BS to MS is called *forward link* and the link from MS to BS is termed as *reverse link*. Forward link communication is one to many i.e. there is one transmitter and many receivers and the reverse link communication is many to one i.e. one receiver receives signals from many transmitters. The channel of a mobile communication system has a tendency to change with time i.e. the impulse response of these channels are time-variant, this is the consequence of the constantly changing physical characteristics of the media. Also the transmitted signal is reflected and refracted by a variety of smooth and rough surfaces, so that it is replicated at the receiver with several time delays. This is called multipath propagation.

### 2.1 Features of fading channels

If we transmit an extremely short pulse over a time-varying multipath channel, the received signal will appear as a train of pulses. Hence one characteristic of a multipath medium is the time spread introduced in the signal that is transmitted through the channel. Now let us consider the transmission of an unmodulated carrier at frequency



$f_c$ , then the low pass equivalent of the received signal is given by[12]

$$r_l(t) = \sum_n \alpha_n(t) e^{-j2\pi f_c \tau_n(t)} = \sum_n \alpha_n(t) e^{-j\theta_n(t)} \quad (2.1)$$

Thus, the received signal consists of the sum of a number of time-variant vectors having amplitudes  $\alpha_n(t)$  and phases  $\theta_n(t)$ . The fading phenomenon is a result of the time variation in the phase  $\theta_n(t)$  i.e. the randomly time varying phase at times results in the vectors adding destructively. The result is that the received signal is very small or practically zero. Thus, the amplitude variation in the received signal is termed as *signal fading* and is due to the multipath characteristic of the channel.

### 2.1.1 Slow and Fast fading

The notion of slow and fast fading is related to the *coherence time*  $T_c$  of the channel, which measures the period of time over which the fading process is correlated. The coherence time  $T_c$  can be defined as [13], the period of time after which the correlation function of two samples of the channel response taken at the same frequency but different time instants drops below a certain predetermined value. The coherence time is also related to the channel *Doppler spread*  $f_d$  by

$$T_c \simeq \frac{1}{f_d} \quad (2.2)$$

The fading is said to be slow if the symbol time duration  $T_s$  is smaller than the channel's coherence time  $T_c$ ; otherwise it is considered to be fast. In slow fading a particular fade level will affect many successive symbols, which leads to burst errors, whereas in fast fading the fading decorrelates from symbol to symbol.

### 2.1.2 Frequency-Flat and Frequency-Selective fading

If all the spectral components of the transmitted signals are affected in a similar manner, then the fading is said to be *frequency nonselective* or *frequency flat*. This is the case for narrowband systems in which the transmitted signal bandwidth is much smaller than the channel *coherence bandwidth*  $W_c$ . This bandwidth measures the frequency range over which the fading process is correlated. It is defined [13] as the frequency

bandwidth over which the correlation function of two samples of the channel response taken at the same time but at different frequencies falls below a suitable value. The coherence bandwidth is related to the *maximum delay spread*  $\tau_{max}$  by

$$W_c \simeq \frac{1}{\tau_{max}} \quad (2.3)$$

Whereas, if the spectral components of the transmitted signals are affected by different amplitude gains and phase shifts, the fading is said to be *frequency selective*. This applies to wideband systems in which the transmitted bandwidth is bigger than the channel's coherence bandwidth.

## 2.2 Modeling of fading channels

When fading affects mobile communication systems, the received carrier amplitude is modulated by the fading amplitude  $\alpha$ , where  $\alpha$  is a random variable (RV) with mean-square value  $\Omega = \bar{\alpha}^2$  and probability density function (PDF)  $p_\alpha(\alpha)$ , which is dependent on the nature of the radio propagation environment. After passing through the fading channel, the signal is affected by additive white Gaussian noise (AWGN), which is assumed to be independent of the fading amplitude  $\alpha$  and is characterized by one-sided power spectral density  $N_o$  (W/Hz). Hence the received signal power is modulated by  $\alpha^2$ . Thus, the instantaneous signal-to-noise power ratio (SNR) per symbol can be defined as  $\gamma = \alpha^2 E_s / N_o$  and the average SNR per symbol by  $\bar{\gamma} = \Omega E_s / N_o$ , where  $E_s$  is the energy per symbol.

The PDF of  $\gamma$  is given by [13]

$$p_\gamma(\gamma) = \frac{p_\alpha(\sqrt{\Omega\gamma/\bar{\gamma}})}{2\sqrt{\gamma\bar{\gamma}/\Omega}}. \quad (2.4)$$

The moment generating function (MGF)  $M_\gamma(s)$  associated with the fading PDF  $p_\gamma(\gamma)$  is defined as

$$M_\gamma(s) = \int_0^\infty p_\gamma(\gamma) e^{s\gamma} d\gamma \quad (2.5)$$

The amount of fading (AF) or *fading figure* associated with the fading PDF is defined as

$$AF = \frac{\text{var}(\alpha^2)}{(E[\alpha^2])^2} = \frac{E[(\alpha^2 - \Omega)^2]}{\Omega^2} = \frac{E(\gamma^2) - (E[\gamma])^2}{(E[\gamma])^2} \quad (2.6)$$

When wideband signals propagate through a frequency-selective channel, their spectrum is affected by the channel transfer function, resulting in a time dispersion of the waveform. This type of fading can be modeled as a linear filter characterized by the following complex valued lowpass equivalent impulse response

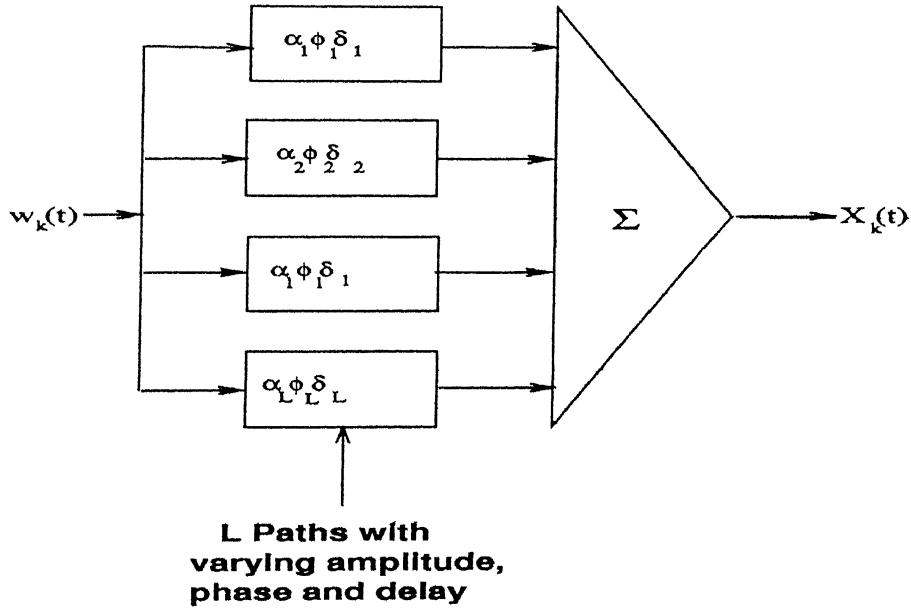


Figure 2.1: Multipath propagation model[3]

$$h(t) = \sum_{l=1}^{L_p} \alpha_l \exp(-j\theta_l) \delta(t - \tau_l) \quad (2.7)$$

Where  $\delta(\cdot)$  is the Dirac delta function,  $l$  the path index, and  $\{\alpha_l\}_{l=1}^{L_p}$ ,  $\{\theta_l\}_{l=1}^{L_p}$ , and  $\{\tau_l\}_{l=1}^{L_p}$  are the random channel amplitudes, phases, and delays, respectively. The model for multipath is shown in Fig. 2.1.

In Eqn. (2.7)  $L_p$  is the number of resolvable paths (the first path being the reference path whose delay  $\tau_1 = 0$ ). Obviously  $L_p$  is related to the ratio of maximum delay spread to the symbol time. Under the slow-fading assumption,  $L_p$  is assumed to be constant over a certain period of time, and  $\{\alpha_l\}_{l=1}^{L_p}$ ,  $\{\theta_l\}_{l=1}^{L_p}$ , and  $\{\tau_l\}_{l=1}^{L_p}$  are all constant over a

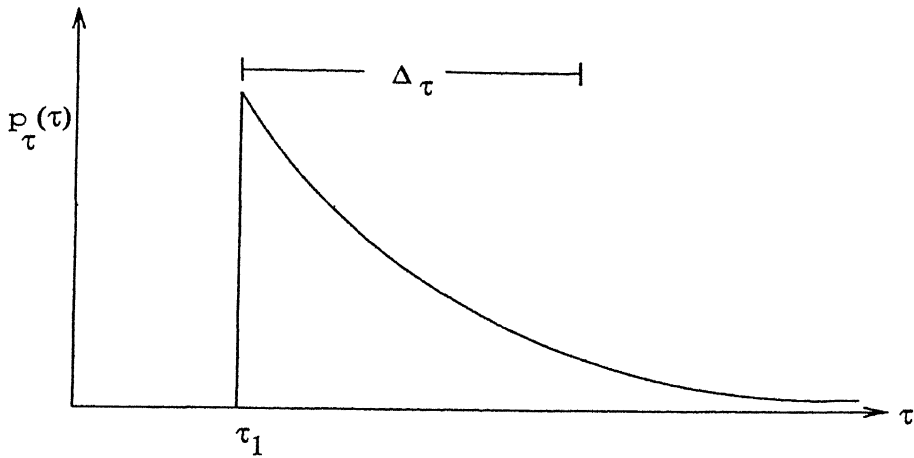


Figure 2.2: The distribution of delays[11]

symbol interval. The fading amplitude  $\alpha_l$  of the  $l^{th}$  resolved path is assumed to be a RV whose PDF be Nakagami-m distributed.

With out loss of generality it can be assumed that the power component decreases with respect to delay, the first arriving path exhibits a lower amount of fading whereas the last arriving path exhibits highest amount of fading. The  $\{\Omega_l\}_{l=1}^{L_p}$  are related to the channel's *power delay profile* (PDP), which is also referred to as the *multipath intensity profile* (MIP) and is decreasing function of delay. The mobile radio channel is well characterized by an exponentially decaying PDP

$$\Omega_l = \Omega_1 \exp(-\tau_l/\tau_{max}), \quad l = 1, 2, \dots, L_p \quad (2.8)$$

where  $\Omega_1$  is the average fading power corresponding to the first (reference) propagation path and  $\tau_{max}$  is the channel maximum delay spread.

The delay spread is defined as the square root of the difference between the mean of the delay squared and the square of the mean delay, which is expressed as[11]

$$\Delta_\tau = \sqrt{\tau^2 - \bar{\tau}^2} \quad (2.9)$$

The delays are often assumed to exponentially distributed [11] shifted by  $\tau_1$  as illustrated by Fig. 2.2. If this distribution is normalized by its delay spread, then it is given by the expression

$$p_\tau(\tau) = \frac{1}{\Delta_\tau} \cdot \exp\left(-\frac{\tau - \tau_1}{\Delta_\tau}\right) \quad (2.10)$$

The mean of the normalized exponential distribution is

$$\bar{\tau} = \frac{1}{\Delta_\tau} \int_{\tau_1}^{\infty} \tau \exp\left(-\frac{\tau - \tau_1}{\Delta_\tau}\right) d\tau = \Delta_\tau + \tau_1 \quad (2.11)$$

The mean square of the distribution is given by

$$\bar{\tau}^2 = \frac{1}{\Delta_\tau} \int_{\tau_1}^{\infty} \tau^2 \exp\left(-\frac{\tau - \tau_1}{\Delta_\tau}\right) d\tau = \Delta_\tau^2 + (\Delta_\tau + \tau_1)^2 \quad (2.12)$$

Thus the standard deviation for a delay with an exponential distribution is

$$\sigma_\tau \triangleq \sqrt{\bar{\tau}^2 - \bar{\tau}^2} = \Delta_\tau \quad (2.13)$$

### 2.2.1 Nakagami-m model

The Nakagami-m PDF is in essence a central chi-square distribution given by [6]

$$p(\alpha) = \frac{2m^m \alpha^{2m-1}}{\Gamma(m) \Omega^m} \exp\left(-\frac{m\alpha^2}{\Omega}\right), \quad \alpha \geq 0 \quad (2.14)$$

where  $m$  is the Nakagami-m fading parameter which ranges from  $\frac{1}{2}$  to  $\infty$ . Fig. 2.3 shows the Nakagami-m PDF for  $\Omega = 1$  and various values of  $m$ -parameter.

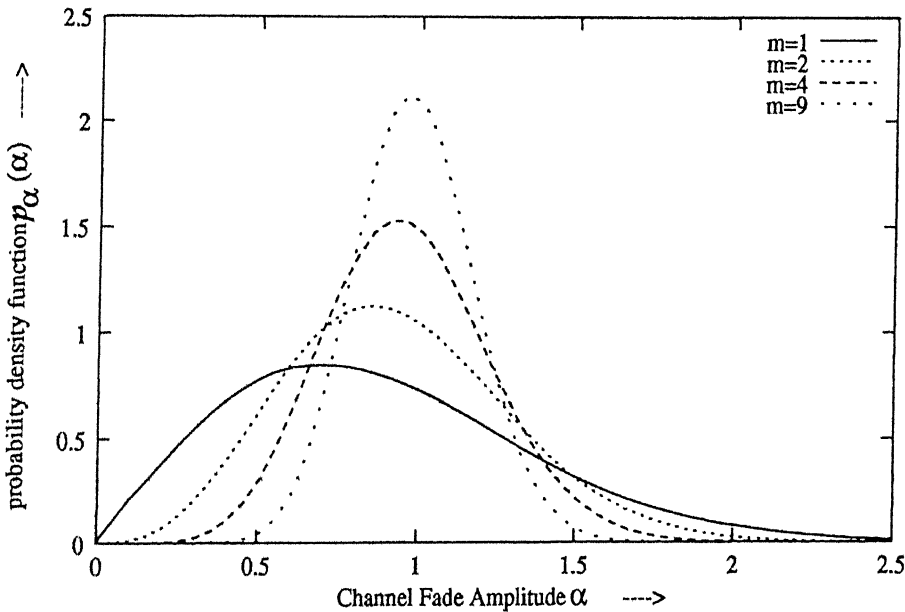


Figure 2.3: Nakagami PDF for  $\Omega = 1$  and various values of the fading parameter  $m$ .

Applying Eqn. (2.4) the SNR per symbol,  $\gamma$ , is distributed according to a gamma distribution given by

$$p_\gamma(\gamma) = \frac{m^m \gamma^{m-1}}{\bar{\gamma}^m \Gamma(m)} \exp\left(-\frac{m\gamma}{\bar{\gamma}}\right), \quad \gamma \geq 0 \quad (2.15)$$

The MGF in this case is given by

$$M_{\gamma}(s) = \left(1 - \frac{s\bar{\gamma}}{m}\right)^{-m} \quad (2.16)$$

and the moments are given by [6]

$$E[\gamma^k] = \frac{\Gamma(m+k)}{\Gamma(m)m^k} \bar{\gamma}^k \quad (2.17)$$

which using Eqn. (2.6) yields an AF of

$$AF = \frac{1}{m}, \quad m \geq \frac{1}{2} \quad (2.18)$$

Hence, the Nakagami- $m$  distribution covers the widest range of fading figure (from 0 to 2) among all the multipath distributions. It includes the one-sided Gaussian distribution ( $m = \frac{1}{2}$ ) and the Rayleigh distribution ( $m = 1$ ) as special cases. In the limit as  $m \rightarrow +\infty$ , the Nakagami- $m$  fading channel converges to a nonfading AWGN channel [13]. Finally, the Nakagami- $m$  distribution often gives the best fit to land-mobile [5, 7] radio link.

### 2.2.2 Characteristics of Nakagami- $m$ distribution

- If the envelope is Nakagami distributed, the corresponding instantaneous power is gamma distributed.
- The parameter  $m$  is also called the 'shape factor' of the Nakagami distribution.
- In the special case  $m = 1$ , Rayleigh fading is recovered, with an 'exponentially distributed' instantaneous power.
- For  $m > 1$ , the variance of random variable reduces as compared to Rayleigh fading.
- Nakagami fading occurs for instance for multipath scattering with relatively large delay-time spreads, with different clusters of reflected waves. Within any one cluster, the phases of individual reflected waves are random, but the delay times are equal for all waves. As a result the envelope of each cumulated cluster signal

is Rayleigh distributed. The average time delay is assumed to differ significantly between the clusters. If the delay times also significantly exceed the bit time of a digital link, the different clusters produce severe intersymbol interference, so the multipath self-interference then approximates the case of co-channel interference by multiple incoherent Rayleigh-fading signals.

- The Nakagami model is also often used to describe the interference cumulated from the multiple independently Rayleigh-fading sources, particularly if these are identically distributed.

## 2.3 Diversity Techniques

Errors in reception tend to occur when the channel is in deep fade i.e. when the channel attenuation is large. If we can supply to the receiver multiple replicas of the same information signal transmitted over independently fading channels, the probability that all the signal components will fade simultaneously is reduced. There are several ways in which we can provide the receiver with multiple independently fading replicas of the same information bearing signal. Depending on the propagation mechanism, these may include:

- **Space diversity**

We may employ a single transmitting antenna and multiple receiving antennas. Usually separation of at least 10 wavelengths is required between two antennas in order to obtain signals that fade independently [12].

- **Frequency diversity**

The same information bearing signal is transmitted on different carriers, where the separation between successive carriers equals or exceeds the coherence bandwidth  $f_c$  of the channel to obtain independently fading signals.

- **Angle of arrival diversity**

If more than one receiving beam oriented towards different non overlapping regions are employed, the signals received via these beams would be decorrelated.

- **Polarization diversity**

This implies a single polarization at the transmitter, with depolarization in the propagation medium. Independent reception is possible with two orthogonal polarizations, and the two resulting signals do not fade in correlated manner.

- **Time diversity**

The same information bearing signal is transmitted in different time slots, where the separation between successive time slots equals or exceeds the coherence time  $T_c$  of the channel to ensure the independence of different fading signals.

- **Multipath diversity**

It can be obtained by using the signal having a bandwidth much greater than the coherence bandwidth of the channel. Such signal will resolve the multipath components and, thus, provide the receiver with several independently fading signal paths. If the signal bandwidth is  $W$  and multipath spread is of  $T_m$  sec, there are  $T_m W$  resolvable components. Since  $T_m \approx \frac{1}{f_c}$ ,  $f_c$  being channel coherence bandwidth, the number of resolvable components may also be expressed as  $W/f_c$ . Hence the order of diversity obtained by using this technique is  $W/f_c$  [12].

Of these, the last two have been primarily considered for digital data transmission. Except for polarization diversity, any number of more-or-less independently fluctuating signals can be made available by multiplication of equipment.

### 2.3.1 Diversity combining techniques

The common linear combining methods that are used are:

- **Selection combining**

This technique is based on choosing the channel with highest SNR and rejecting all others. Fig. 2.4 shows the schematic diagram for this technique.

- **Equal gain combining (EGC)**

In this case the decision statistics from all the  $L$  channels are combined with equal gain for final detection. The combiner is a post-detection combiner. Fig. 2.4 gives the details for this technique.



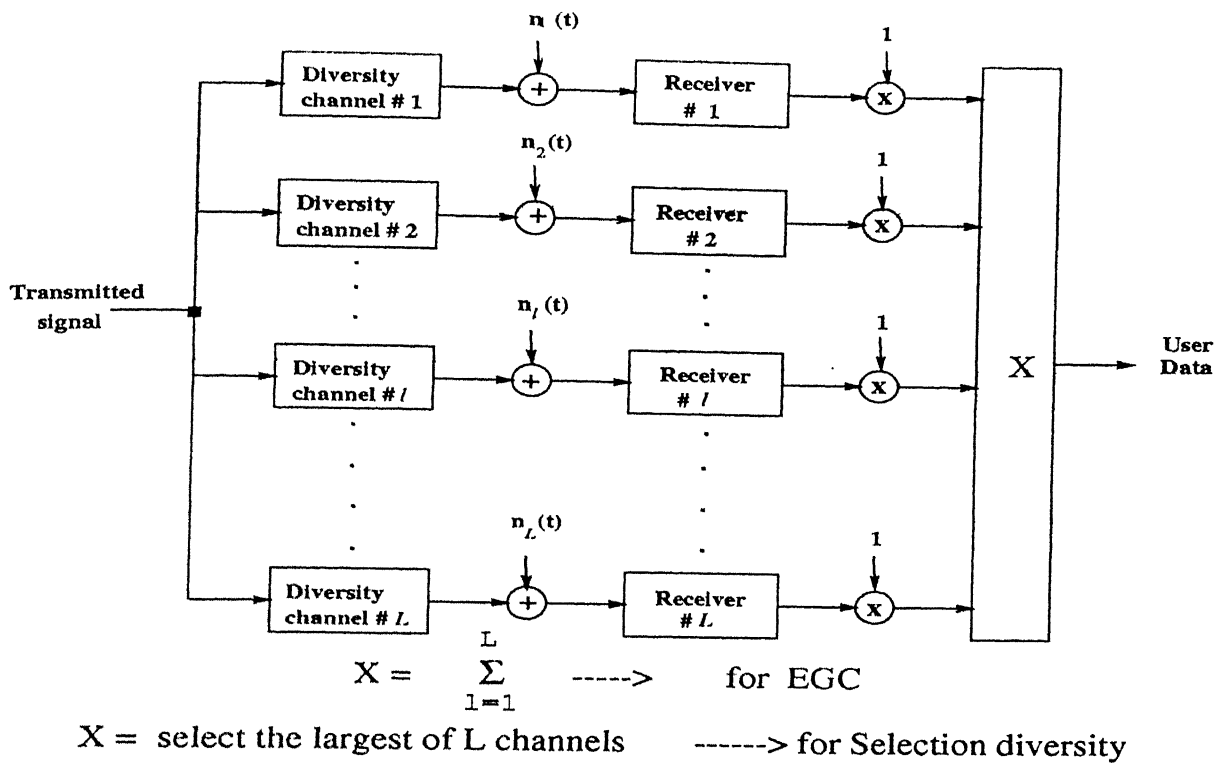


Figure 2.4: Block diagram for EGC and selection combining techniques [11]

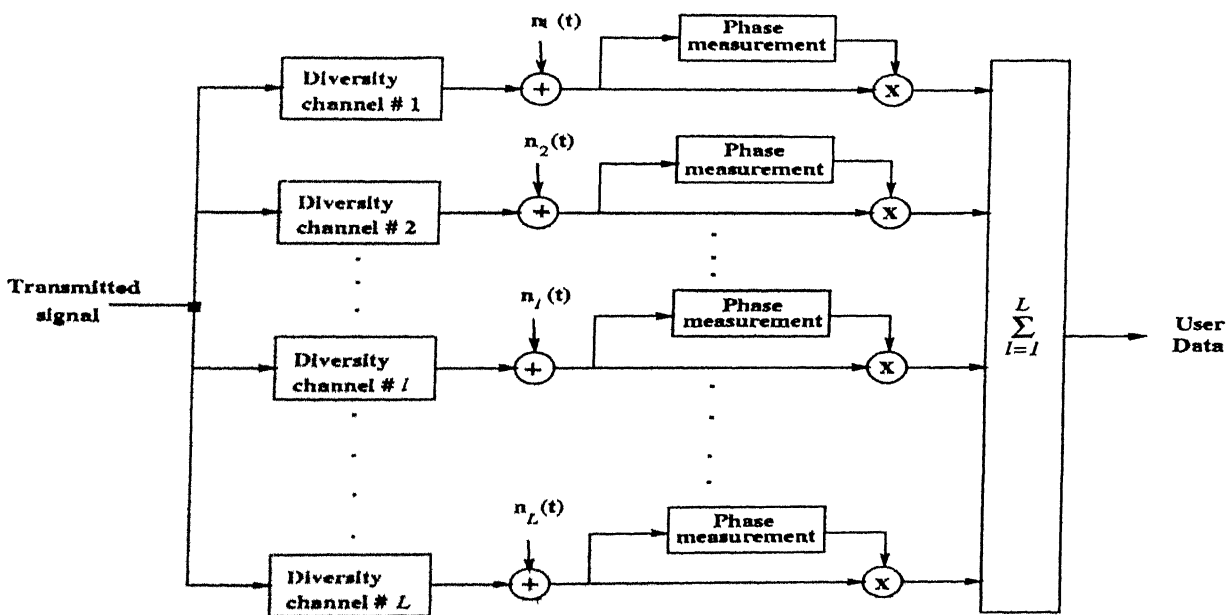


Figure 2.5: Block diagram for MRC technique [11]

- **Maximal ratio combining (MRC)**

The phases of the diversity signals from  $L$  channels being added together are aligned and their envelopes are weighted in proportion to the square roots of their SNR's [11]. This is the optimal combining technique as it yields the maximum achievable SNR. Block diagram for this technique is shown in Fig. 2.5 .

# Chapter 3

## Downlink Analysis

When the spread spectrum employs pseudo random sequence with chip time  $T_c$ , inversely proportional to the spreading bandwidth, the individual paths can be distinguished if they are mutually separated by delays greater than  $T_c$ . Since in this case the various delayed versions of the signal will be mutually nearly uncorrelated. Received signal of  $k^{th}$  user[3]

$$X_k(t) = \sqrt{E_c(k)} \sum_n x_n(k) \times \sum_{l=1}^L \alpha_l h(t - nT_c - \delta_l) \times \left\{ a_n^{(I)}(k) \cos [2\pi f_0(t - \delta_l) + \phi_l] + a_n^{(Q)}(k) \sin [2\pi f_0(t - \delta_l) + \phi_l] \right\} \quad (3.1)$$

where,  $E_c$  is the energy per chip of the data,  $x_n(k)$  is the  $n$ th symbol bit of the  $k$ th user,  $\alpha_l$  is the attenuation of the  $l$ th path,  $h(.)$  is the baseband wave shaping filter impulse response,  $\delta_l$  is the delay of the  $l$ th path,  $\phi_l$  is the phase of the  $l$ th path signal,  $a_n^{(I)}(k)$  and  $a_n^{(Q)}(k)$  is the in phase and quadrature PN sequence of the user.

Each of the distinguishable multipath components will actually be a linear combination of several indistinguishable multipaths of varying amplitudes. Since these will add as random vectors, the amplitude of each term will appear to be Nakagami-m distributed and the phase uniformly distributed.

Let  $X_0(t)$  be the unmodulated pilot signal so that  $x_n(0) = 1$  for all  $n$ . We assume that the pilot pseudo random sequence is shared by all users. Hence the received signal containing  $K_u$  users and a pilot sequence, all originating from the same Base station

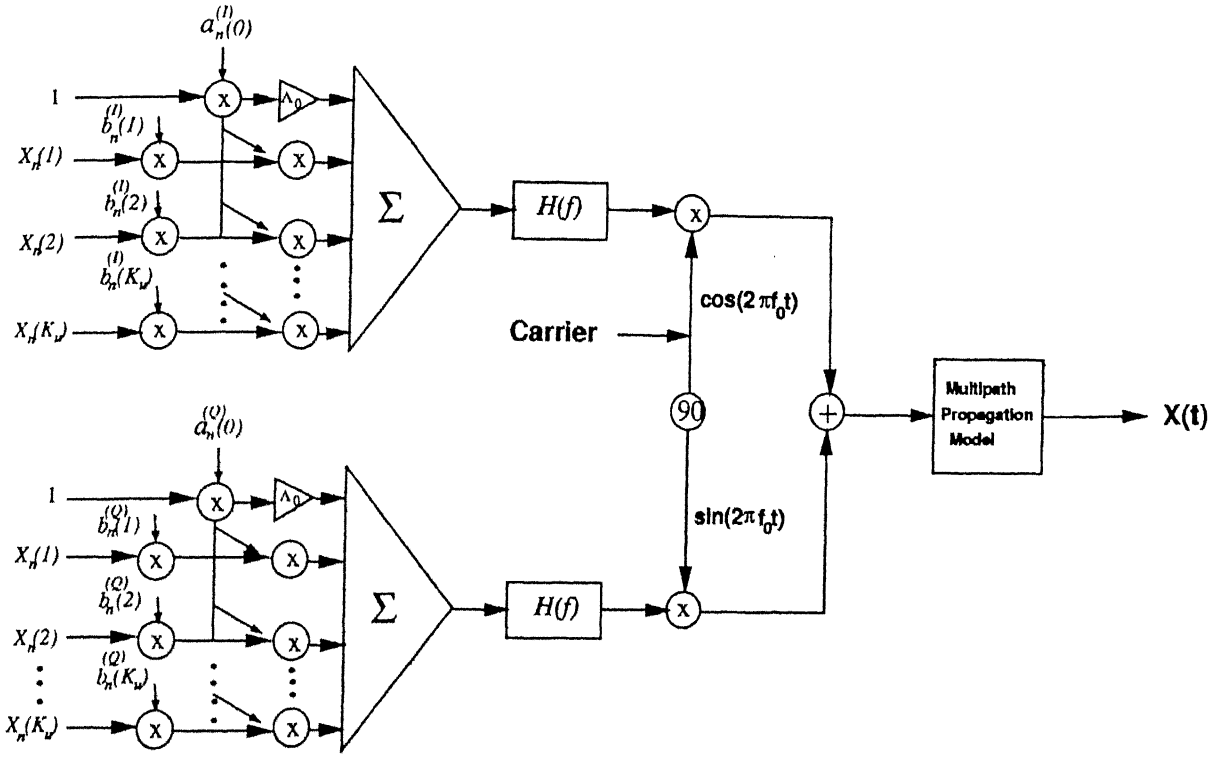


Figure 3.1: Multiuser modulator and multipath channel[3]

will be (Fig. 3.1)

$$X(t) = X_0(t) + \sum_{k=1}^{K_u} X_k(t) \quad (3.2)$$

$X_0(t)$  is further scaled by  $A_0$ , the additional gain allotted the pilot signal.  $a_n^I(0)$  and  $a_n^Q(0)$  are pilot's QPSK spreading sequences. The users sequences are the products of those of the pilot and of the user-specific sequences  $b_n^I(k)$ ,  $b_n^Q(k)$  i.e.

$$a_n^I(k) = a_n^I(0).b_n^I(k), \quad a_n^Q(k) = a_n^Q(0).b_n^Q(k) \quad (3.3)$$

The timings of all individual users is locked to that of the pilot sequence, so that multipath delays need only be searched on the pilot sequence.

The delays of different multipath components are estimated. Then it is used to remove pilot QPSK spreading, giving rise to the quadrature outputs

$$\sqrt{E_c}.[A_0 + x_n(k).b_n^I(k)].\alpha_l \cos(\phi_l) + \nu_n^I \quad (3.4)$$

$$\sqrt{E_c}.[A_0 + x_n(k).b_n^Q(k)].\alpha_l \sin(\phi_l) + \nu_n^Q \quad (3.5)$$

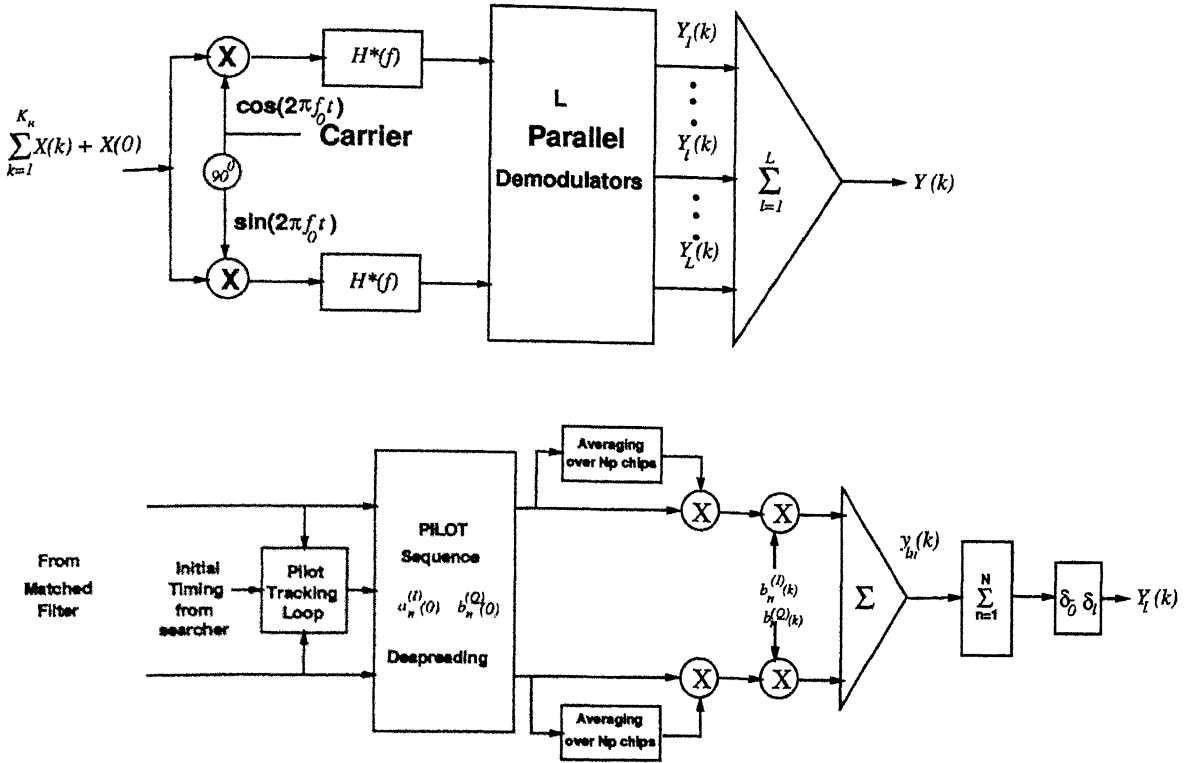


Figure 3.2: Rake demodulator for multipath propagation[3]

$A_0$  is the pilot gain,  $\nu_n^I$  and  $\nu_n^Q$  are the contribution of all other (uncorrelated) multipath components as well as those of all other users. From these outputs the relative path values  $\alpha_l \cos \phi_l$  and  $\alpha_l \sin \phi_l$  can be estimated by simply averaging over an arbitrary number of chips  $N_p$ . This number should be as large as possible without exceeding the period over which  $\alpha_l$  and  $\phi_l$  remain relatively constant.

The result of  $n^{\text{th}}$  chip of the  $l^{\text{th}}$  path, after multiplication by the quadrature-user-specific pseudorandom sequences as shown in Fig. 3.2, is

$$y_{ln}(k) = \sqrt{E_c} x_n(k) \hat{\alpha}_l \alpha_l \cos(\phi_l - \hat{\phi}_l) + \hat{\alpha}_l (\nu_n^{(I)} \cos \hat{\phi}_l + \nu_n^{(Q)} \sin \hat{\phi}_l) \quad (3.6)$$

Summing over the  $N$  chips over which  $x_n(k)$  is constant ( $\pm 1$ ), we have

$$Y_l(k) = \pm N \sqrt{E_c} \alpha_l \hat{\alpha}_l \cos(\phi_l - \hat{\phi}_l) + \hat{\alpha}_l [\cos \hat{\phi}_l \sum \nu_n^{(I)} + \sin \hat{\phi}_l \sum \nu_n^{(Q)}] \quad (3.7)$$

Thus,

$$E[Y_l(k) | x_n(k) = -1] = -N [\sqrt{E_c} \alpha_l \hat{\alpha}_l \cos(\phi_l - \hat{\phi}_l)], \quad (3.8)$$

with a change of sign if  $x_n(k) = 1$ , and

$$\text{Var}[Y_l(k)] = N\hat{\alpha}_l^2 I_0/2 \quad (3.9)$$

where  $I_0$  is given by  $I_0 = N_0 + \sum_{j=1}^{K_u} E_c(j)$ .

### 3.1 Probability of Error for Nakagami-m channel

Assuming that each path's attenuation is uncorrelated to that of others, the multipath component amplitudes be RV's mutually independent, then the error probability for perfect estimates is given by [3]

$$\begin{aligned} P_E &= E(P_E[\alpha_1, \alpha_2, \dots, \alpha_L]) < E[\prod_{l=1}^L \exp(-\alpha_l^2 N E_c / I_0)] \\ &= \prod_{l=1}^L E[\exp(-\alpha_l^2 E_s / I_0)] \triangleq \prod_{l=1}^L Z_l \triangleq Z. \end{aligned} \quad (3.10)$$

Here,  $E_s \triangleq N E_c$  is the  $N$ -chip symbol energy, and expectations are with respect to the random variables  $\alpha_l$ .

Taking  $\alpha_l$  variable to be Nakagami- $m$  distributed the PDF of  $\alpha_l$  is given by (2.14), which is being reproduced here

$$p(\alpha_l) = \frac{2m^m \alpha_l^{2m-1}}{\Gamma(m) \Omega_l^m} \exp(-\frac{m\alpha_l^2}{\Omega_l}), \quad \alpha_l \geq 0. \quad (3.11)$$

where  $\Omega_l = E[\alpha_l^2]$  and letting  $\beta_l = \alpha_l^2$ , we obtain

$$\begin{aligned} p(\beta_l) &= \frac{p(\alpha_l)|_{\alpha_l=\sqrt{\beta_l}}}{\frac{d\beta_l}{d\alpha_l}|_{\alpha_l=\sqrt{\beta_l}}} \\ &= \frac{m^m \beta_l^{m-1} \exp(-m\beta_l/\Omega_l)}{\Omega_l^m \Gamma(m)}, \quad \beta_l \geq 0. \end{aligned} \quad (3.12)$$

Thus, for Nakagami- $m$  distributed attenuations,

$$\begin{aligned} Z_l &= E[e^{-\frac{\beta_l E_s}{I_0}}] \\ &= \frac{m^m}{\Gamma(m)} \int_0^\infty \beta_l^{m-1} e^{-\beta_l(m+E_s/I_0)} d\beta_l \\ &= \frac{1}{(1 + \frac{\Omega_l E_s}{m I_0})^m} \end{aligned} \quad (3.13)$$

Hence, the probability of error for  $L$  multipaths assuming all paths having equal average strength (i.e  $\Omega_l = \Omega, \forall l$ ) is

$$\bar{P}_E < Z \triangleq \prod_{l=1}^L Z_l = \frac{1}{(1 + \frac{\bar{E}_s}{mI_o})^{mL}} \quad (3.14)$$

Where  $\bar{E}_s = \Omega E_s$ . Eqn. (3.14) is the Chernoff bound on probability of error for Nakagami-m channel.

Using MGF approach [13], the average BER for QPSK is given by

$$\bar{P}_E = \frac{1}{\pi} \int_0^{3\pi/4} \prod_{l=1}^L M_{\gamma_l}(-\frac{1}{2\sin^2\phi}) d\phi \quad (3.15)$$

where  $M_{\gamma_l}(\cdot)$  is given by (2.16) for Nakagami-m distribution, and  $\bar{\gamma}_l = \frac{\Omega E_s}{I_o}$ . Hence, the average probability of error is given by the expression

$$\bar{P}_E = \frac{1}{\pi} \int_0^{3\pi/4} (1 + \frac{\Omega E_s}{2mI_o \sin^2\phi})^{-mL} d\phi \quad (3.16)$$

An upper bound on (3.16) can be obtained by evaluating the integrand at  $\phi = \pi/2$ , as integrand has a single maximum at this value.

$$\bar{P}_E \leq \frac{3}{4} (1 + \frac{\Omega E_s}{2mI_o})^{-mL} \quad (3.17)$$

# Chapter 4

## Simulation Methodology

This simulation has been carried out to evaluate the performance of forward link of DS-CDMA (IS-95 standard) over Nakagami-m channel. The assumptions made in the simulation are:

- The delays of multipath do not vary significantly during the life of one call.
- The fading parameters i.e. attenuation and phase remain nearly constant over one symbol duration.
- The value of fading parameter  $m$  for Nakagami-m channel is assumed to be same for all the multipaths.
- It has been assumed that the local oscillator at the receiver is synchronized with the transmitter.
- The delay of each of the multipaths is known to receiver i.e. it has been assumed that the chip time of PN sequence has been acquired.

### 4.1 Transmitter

The transmitter of Fig. 3.1 has been implemented. The block diagram for IS-95 single-user transmitter is shown in Fig. 4.1. The implementation steps are as follows:



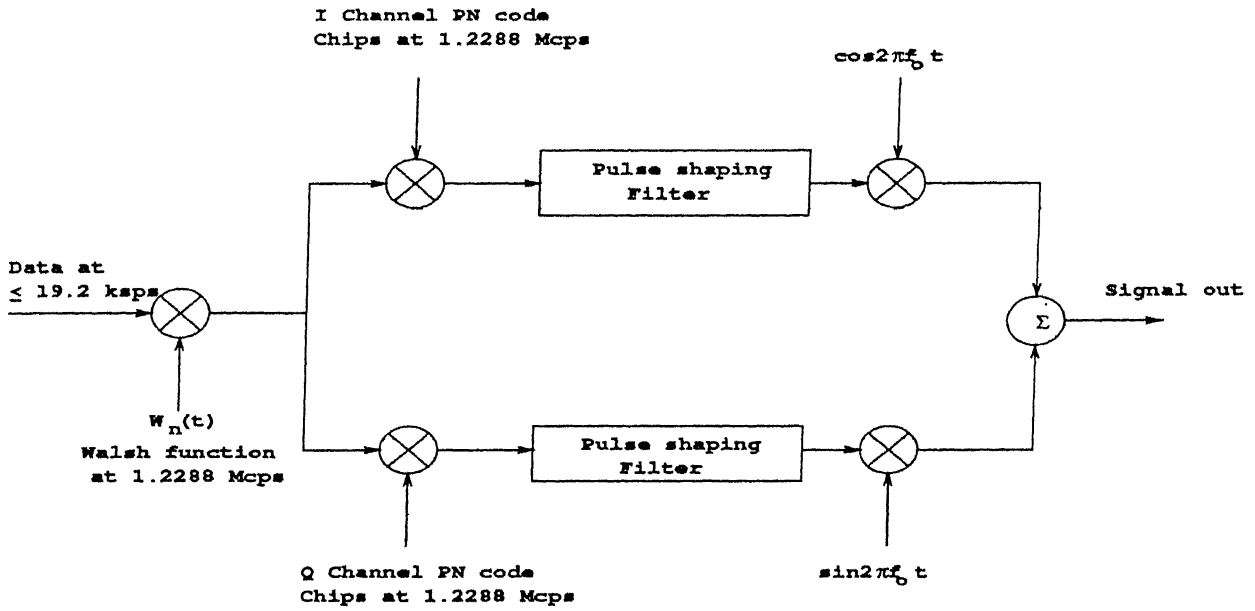


Figure 4.1: Block diagram of transmitter for single-user [11]

- The input bit stream consisting of plus one's and minus one's (+1 and -1) has been generated using random number generator with uniform distribution.
- The Walsh function for 64 ( $N=32$ ) chip length has been generated by [11]

$$[H_{2N}] = \begin{bmatrix} H_N & H_N \\ H_N & -H_N \end{bmatrix} \quad (4.1)$$

The basic building block representing logic elements  $\{0,1\}$  as  $\{1,-1\}$  is

$$[H_2] = \begin{bmatrix} 1 & 1 \\ 1 & -1 \end{bmatrix} \quad (4.2)$$

- The characteristic polynomials of in-phase and quadrature PN sequences are given by [11]

$$\begin{aligned} f_I(x) &= 1 + x^2 + x^6 + x^7 + x^8 + x^{10} + x^{15} \\ f_Q(x) &= 1 + x^3 + x^4 + x^5 + x^9 + x^{10} + x^{11} + x^{12} + x^{15} \end{aligned} \quad (4.3)$$

These in-phase and quadrature sequences are generated by mechanizing the binary primitive polynomials Eqn. (4.3) as simple shift register generators (SSRG) configuration as shown in Fig. 4.2. The initial vector of the registers in the figure

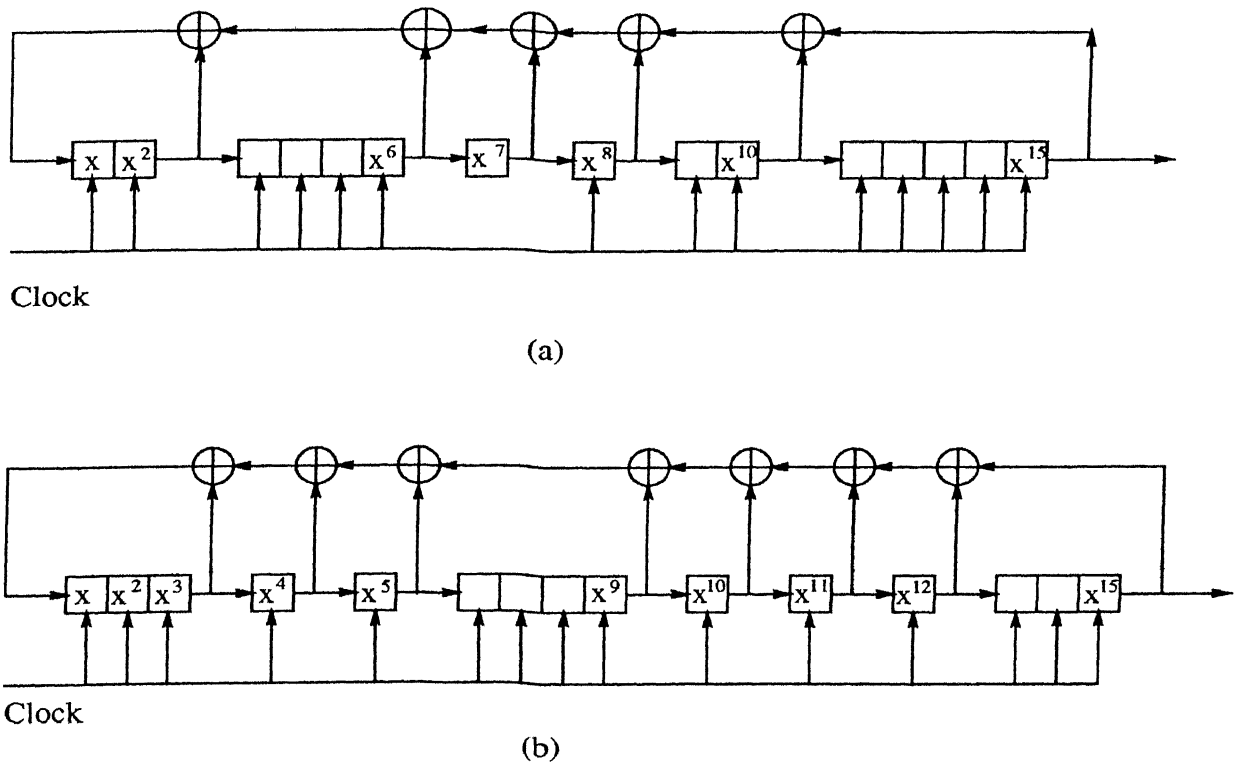


Figure 4.2: SSRG configuration for generation of (a) In-phase PN sequence (b) Quadrature PN sequence [11]

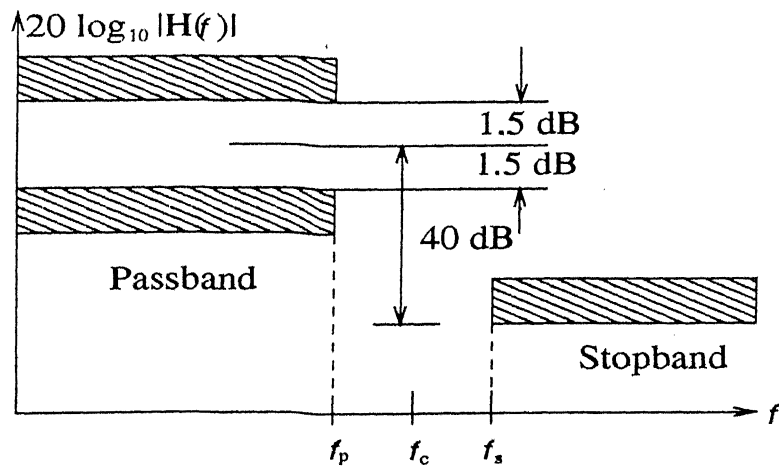


Figure 4.3: FIR Filter specifications [11]

is 0000000000000001. The length of each PN sequence is  $2^{15} - 1 = 32767$ . One zero bit is added at the end of the largest runlength of (14) zeros in order to make the length of PN sequences equal to 32768. In IS-95 this has been done to have exactly 75 cycles of the sequences in 2 secs, as the clock rate is 1.2288 Mcps.

- The data bits are modulated by the channel assigned Walsh sequence resulting 64 chips (at the rate of 1.2288 Mcps) per bit. Then the Walsh coded data bits are modulated by I and Q phase PN sequence, with particular offset which identifies the base station, we get chips at the rate of 1.2288 Mcps at the output of PN sequence modulator. These chips are convolved with the coefficients of FIR filter to shape the baseband pulse. The filters are specified to have a frequency response  $H(f)$  that satisfies the limits shown in Fig. 4.3. The filter coefficients are given in Table 4.1[11] and impulse response is shown in Fig. 4.4.
- The baseband waveform is then carrier modulated for QPSK modulation.

## 4.2 Channel

Simulation of the multipath channel model is carried out in accordance with the Fig. 4.5. It has been assumed that each path constitutes several discrete paths, as a result the envelope of each path is Nakagami-m distributed [9].

### 4.2.1 simulation steps for $m \geq 1$

- Select an appropriate value of the m parameter.
- Generate m exponentially distributed random variables  $(Y_1, Y_2, \dots, Y_m)$ , by first generating m uniform random variables  $(X_1, X_2, \dots, X_m)$  using the random function, and then taking  $Y_i = -\log(X_i)$  for  $i = 1, 2, \dots, m$ .
- Average  $Y = (Y_1 + Y_2 + \dots + Y_m)/m$ , then Y is gamma distributed.
- Take the square root of Y,  $Z = \sqrt{Y}$ , where Z will be Nakagami-m distributed.

$n$	$h_0(n)$	$n$	$h_0(n)$
0, 47	-0.025288315	12, 35	0.007874526
1, 46	-0.034167931	13, 34	0.84368728
2, 45	-0.035752323	14, 33	0.126869306
3, 44	-0.016733702	15, 32	0.094528345
4, 43	0.021602514	16, 31	-0.012839661
5, 42	0.064938487	17, 30	-0.143477208
6, 41	0.091002137	18, 29	-0.211829088
7, 40	0.081894974	19, 28	-0.140513128
8, 39	0.037071157	20, 27	0.094601918
9, 38	-0.021998074	21, 26	0.441387140
10, 37	-0.060716277	22, 25	0.785875640
11, 36	-0.051178658	23, 24	1.000000000

Table 4.1: Coefficients of FIR filter [11]

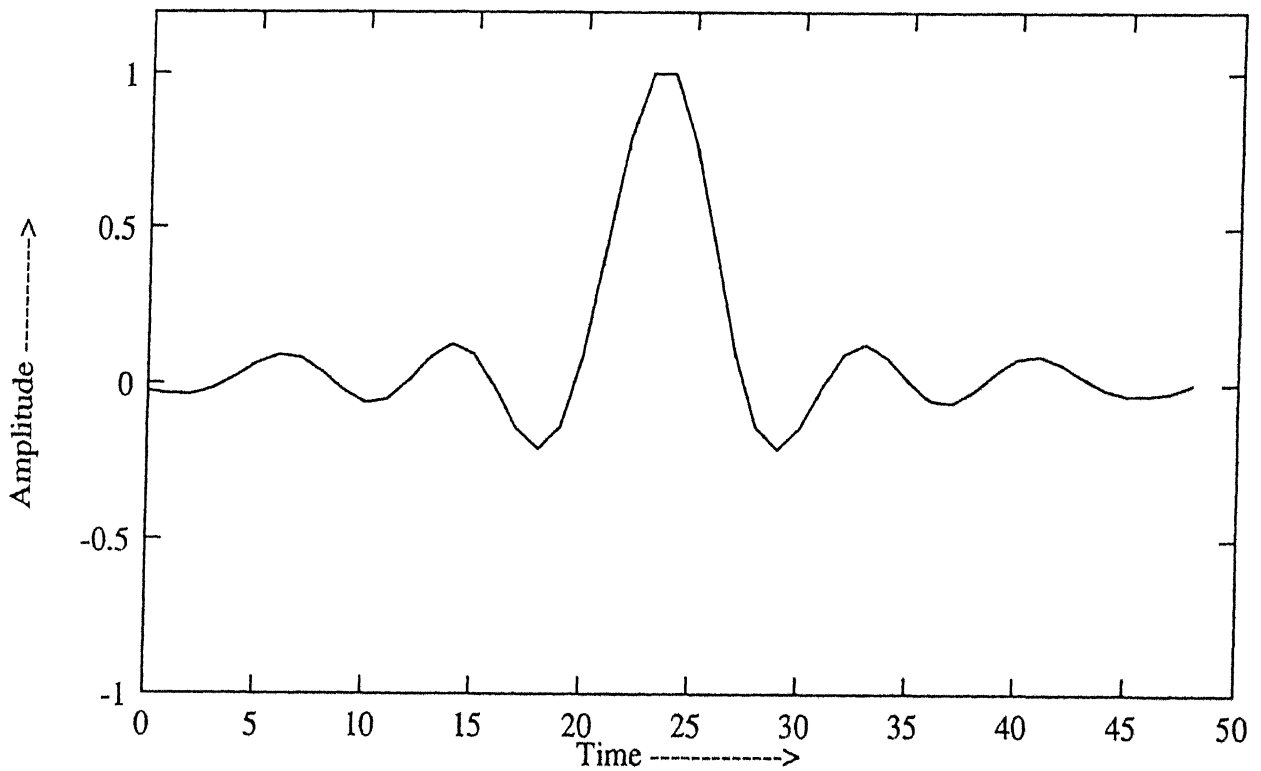


Figure 4.4: Impulse response of FIR filter [11]

### 4.2.2 simulation steps for $m < 1$

Rayleigh distribution has been shown by many investigators, to be appropriate for modeling the fading statistics of a channel. However, it is possible that fading becomes more severe than Rayleigh fading as a result of high variability in the channel. The channel measurement results observed by Nakagami [11] indicate that the Nakagami- $m$  distribution with  $m$  in the range of  $0.5 \leq m < 1$  is useful for modeling the fading characteristic of a channel when the fading is more severe than Rayleigh fading.

Let  $z(t) = r(t)e^{j\theta(t)}$  be a wide-sense stationary (WSS) complex random process that is characterized by the autocorrelation function

$$R_z(\Delta t) = E[z(t)z_*(t + \Delta t)] \quad (4.4)$$

and satisfies the following properties.

1.  $r(t)$  is Nakagami- $m$  distributed with the second moment  $\Omega = R_z(0)$  and the fading parameter  $m$  limited in the range  $m \in [0.5, 1)$ .
2.  $\theta(t)$  is uniformly distributed over  $[0, 2\pi)$ .
3.  $r(t)$  and  $\theta(t)$  are mutually independent.

Then  $z(t)$  can be represented by [15]

$$z(t) = \mu(t)w(t) \quad (4.5)$$

where  $\mu(t)$  is a WSS nonnegative random process and  $\mu^2(t)$  follows a standard beta distribution with parameters  $m$  and  $1-m$ , and  $w(t)$ , being independent of  $\mu(t)$ , is a zero-mean WSS complex Gaussian process with an autocorrelation function

$$R_w(\Delta t) = E[w(t)w^*(t + \Delta t)] \quad (4.6)$$

satisfying  $R_w(0) = \Omega/m$ .  $R_z(\Delta t)$  and  $R_w(\Delta t)$  are related by

$$R_z(\Delta t) = R_\mu(\Delta t).R_w(\Delta t) \quad (4.7)$$

Where  $R_\mu(0) = m$ . The representation of  $z(t)$  by 4.5 is the desired simulation model. The simulation steps for the above model are [15]:

- $\mu(t)$  can be generated by  $\mu(t) = F^{-1}(\Phi(y(t)))$ , where,  $y(t)$  is a zero-mean unit variance Gaussian process with autocorrelation function  $\rho(\Delta t) = E[y(t)y(t+\Delta t)]$ ,  $\Phi(y(t))$  is the CDF of  $y(t)$ , and  $F(x) = I_{x^2}(m, 1-m)$ ,  $0 \leq x \leq 1$ , where,  $I_u(a, b)$  is the incomplete beta function.  $y(t)$  is generated by using Rice's sum of sinusoids [16].
- $w(t)$  is generated independently by separately generating in-phase and quadrature-phase components based on the sum of sinusoids method.
- $z(t)$  is then generated by multiplying  $\mu(t)$  and  $w(t)$  as in Eqn. 4.5

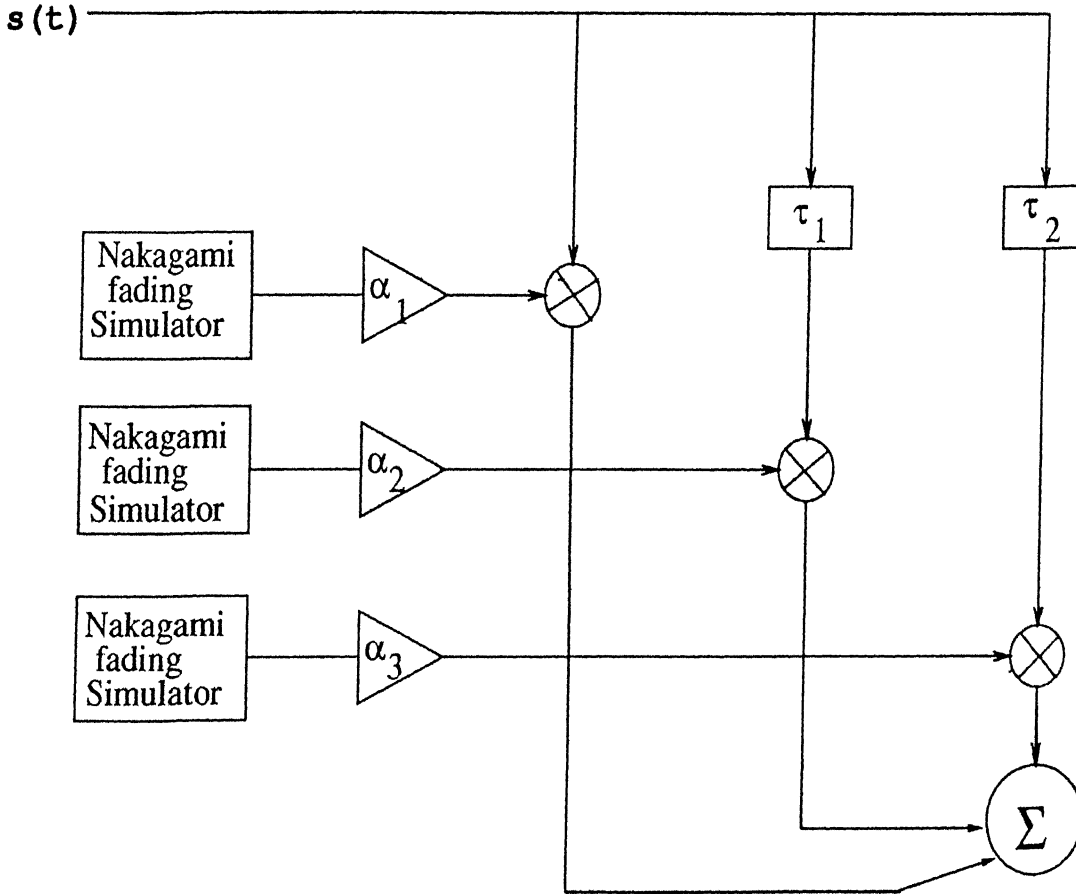


Figure 4.5: Simulation model for Nakagami-m fading channel

### 4.3 Receiver

The Nakagami-m channel model has been used to generate the received signal given by Eqn. (3.1) for multipath propagation as per the channel shown on Fig. 4.5. In the figure  $\alpha$  is the attenuation coefficient and  $\tau_i$  is the time delay for  $i^{th}$  path. The number of multipaths are taken to be 3 (same as IS-95 standard). The receiver block diagram is shown in Fig. 3.2.

The steps followed for simulation are:

- The received signal is carrier demodulated and then passed through the matched filter. The transfer function of the matched filter is complex conjugate of the filter used in transmitter. Since the filter response is symmetrical and real the response of matched filter is also same. Hence the same coefficients as shown in Table 4.1 are used in the receiver.
- The matched filter output is then fed to a demodulator which is combination of  $L$  parallel demodulators ( $L=3$  in this case).
- It has been assumed that the multipath delays are known to the receiver, hence each demodulator despreads the received signals of each multipath independently by correlating it with the I and Q PN sequences. Then the despread signal is averaged over a varying number of chips ( $N_p$ ) to estimate the relative path values (i.e.  $\alpha_i \cos \phi_i$  and  $\alpha_i \sin \phi_i$ ) on the I-phase and Q-phase branches of Fig. 3.2. The value of  $N_p$  should be less than or equal to the number of chips over which the attenuation and phase remains constant.
- The estimated path values are multiplied with the despread signal. Then the correlation with the Walsh sequence is carried out. The resulting signal from I-phase and Q-phase are added followed by summing the successive chips over a symbol duration of 64 chips .

In this simulation the performance of the forward link is studied over varying channel. This change in channel has been affected by changing the value of fading parameter  $m$ .



# Chapter 5

## Results and Conclusion

Simulation of forward link of IS-95 standard has been carried out to study its performance over Nakagami- $m$  channel. The number of resolvable multipaths is taken to be 3 as specified in IS-95 standard. Nakagami- $m$  channel model is considered to be a better model for mobile channel conditions, as it includes Rayleigh fading channel ( $m=1$ ), one-sided Gaussian channel ( $m=0.5$ ) and in the limit  $m \rightarrow +\infty$ , non fading AWGN channels as special cases. Therefore, it is expected that the performance curves obtained will be more general. The transmitter and receiver have been implemented as per the block diagrams given in Fig. 3.1 and Fig. 3.2 respectively. Plots have been obtained for bit error rate (BER) vs. signal to noise ratio (SNR) under various channel conditions.

In this work zero padded PN codes have been used as was discussed in section 4.1. Fig. 5.1 shows that the autocorrelation function is not much effected by padding a zero in the PN sequence. Also it is shown in Fig. 5.2 that zero padding does effects the autocorrelation function if the total length of PN sequence is less.

The observations from results obtained by the simulations are as follow:

- Case 1:  $m < 1$

A channel with more obstructions, such as in urban areas, can be more appropriately modeled with Nakagami- $m$  channel with  $m < 1$  as compared to Rayleigh channel, which has been generally used to model such channels. Fig. 5.3 shows the BER vs. SNR curves that have been plotted for  $m = 0.5, 0.7$  and  $1.0$  respec-

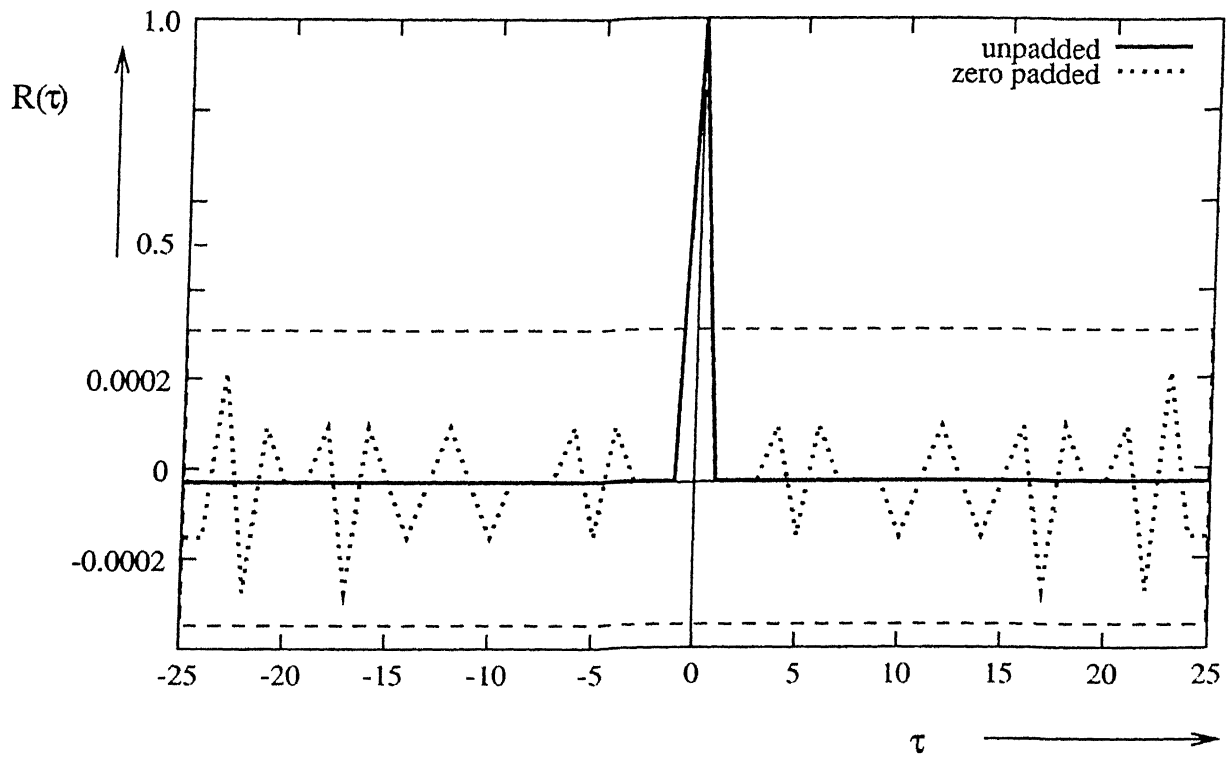


Figure 5.1: Autocorrelation function of I-phase PN code

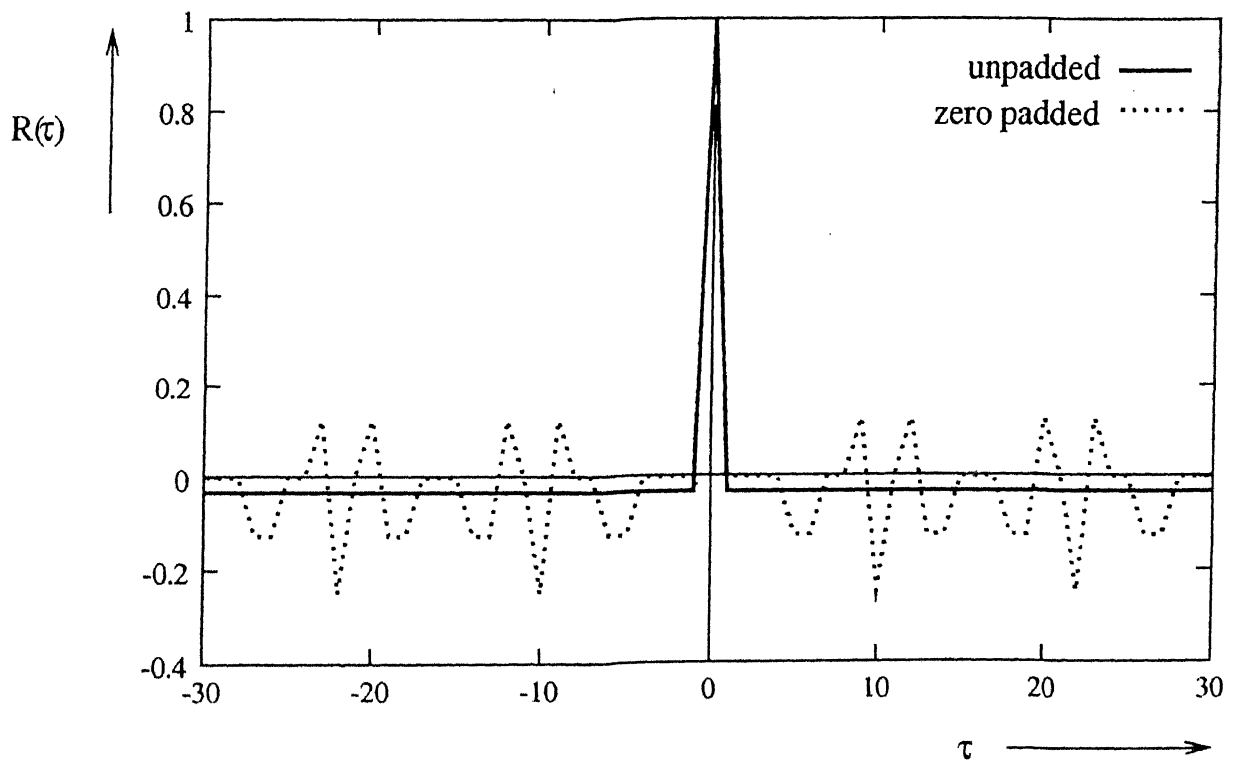


Figure 5.2: Autocorrelation function PN code of length 15.

tively. It also shows the Chernoff bound (Eqn. 3.14) for BER for  $m = 0.5$ . It can

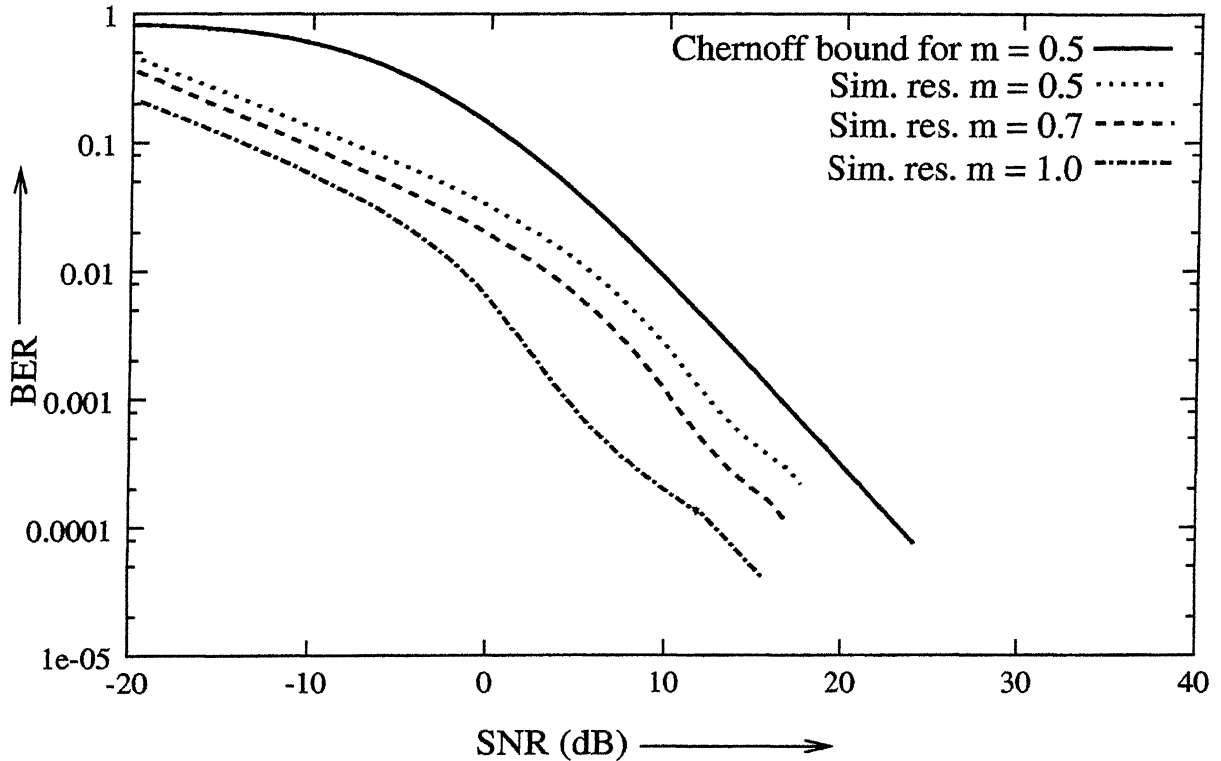


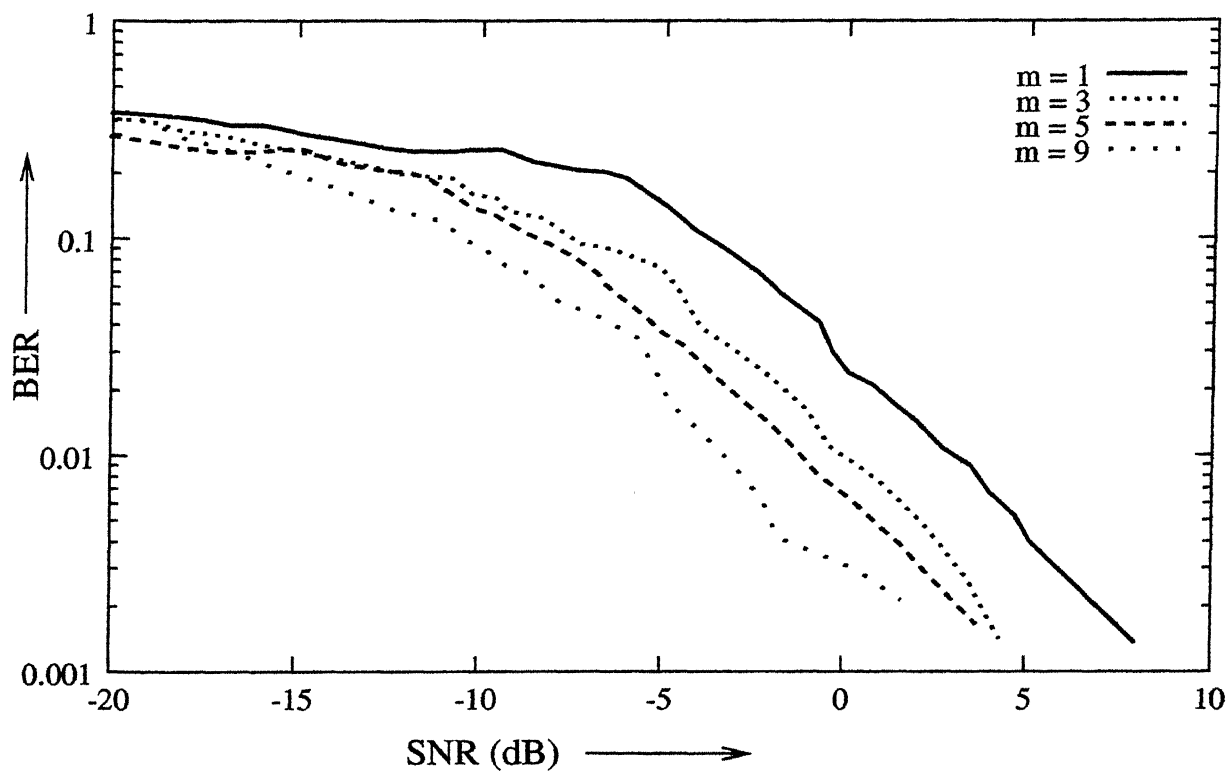
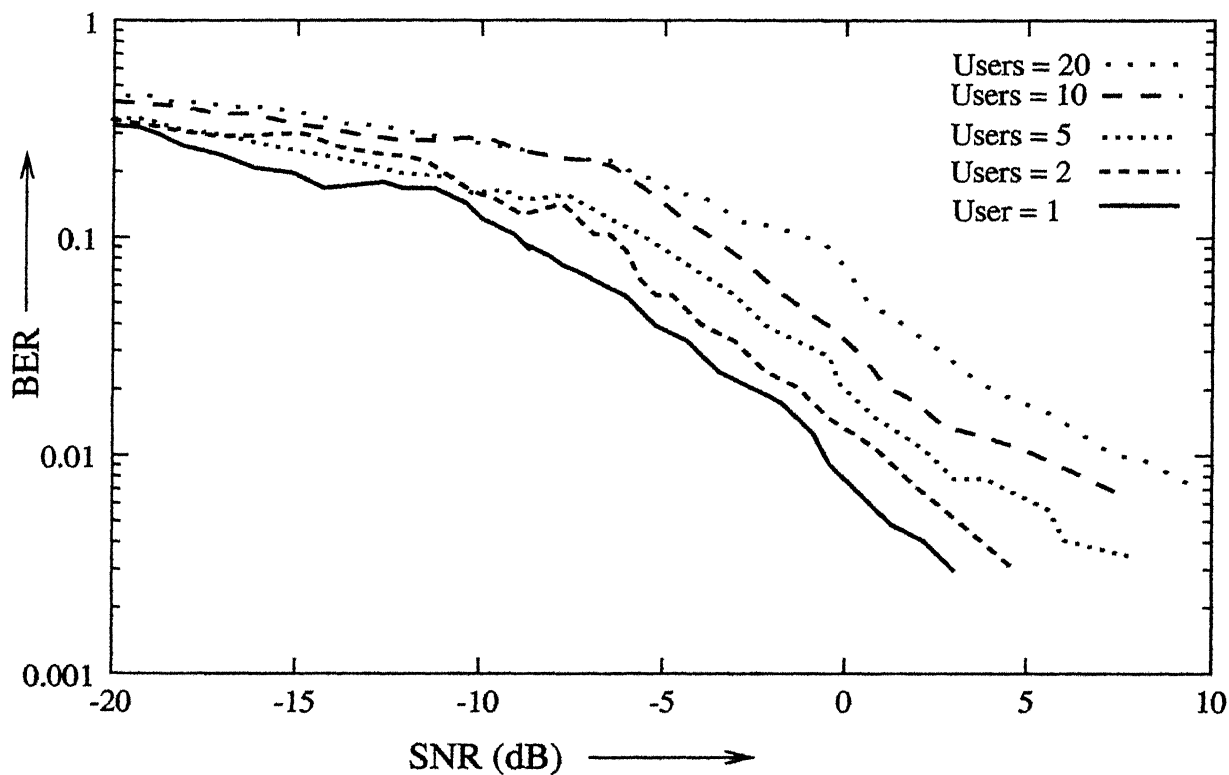
Figure 5.3: Simulation results for  $m = 0.5, 0.7$  and  $1.0$

be clearly seen that the curves are well below the bound and the increase in value of  $m$  results in decrease in BER. This agrees with the notion of Nakagami- $m$  distribution that the increase in value of  $m$  reduces the variance. It can also be seen that for  $m < 1$  the performance is not as good as  $m = 1$  (Rayleigh fading channel). This is again in conformity with the fact that Nakagami- $m$  channel with  $m < 1$  is worse when compared to Rayleigh fading channel.

#### Case 2: $m > 1$

Nakagami- $m$  model with  $m > 1$  is a better model for suburban/rural areas, as the increase in value of  $m$  implies that the number of scatterers in the medium is reduced. Fig. 5.4 shows curves for different values of  $m = 1, 3, 5$  and  $9$ . The curves agree with the fact that with increase in  $m$  the performance gets better.

- In Fig. 5.5 the curves for varying number of users, for the case when  $m = 3$ , have been plotted. It can be observed that as the number of users increase BER also increases. But this increase is nominal because of the orthogonality between

Figure 5.4: Simulation results for  $m=1, 3, 5$  and  $9$ Figure 5.5: Results for  $m=3$  with varying number of users

# Chapter 1

## Introduction

With the spectacular growth in the communication facilities, the demand of high data rate is increasing day by day. Most of the communication techniques have used single carrier modulation to transmit the data, which needs complicated equalizer blocks at the receiver to nullify the impairment made by channel. Though almost no communication system runs without equalizers, but we always try to minimize their need as they are highly complicated blocks. Normally more is the data rate, more complicated the equalizer is. Hence comes the idea of transmitting high speed data occupying large bandwidth by dividing into several low speed data streams occupying smaller bandwidth. To do so, we transmit many data streams on frequency division multiplexed subcarriers. Hence the equalizer needed becomes less complicated and sometimes it is completely eliminated. The systems based on this idea are put under the family of multicarrier systems.

### 1.1 Few implementations of multicarrier systems

The principle of multicarrier was originally applied in Collins' Kineplex Systems in [4]. There are claims of even early implementations. It has since been called by many names and used with varying degree of success in different media, e.g.[8]

- FDM telephony group band modem.
- Telephony voice band modem.
- Upstream cable modem.

users specific codes.

- Fig. 5.6 shows the Chernoff bound and simulation result for Rayleigh fading channel. This plot shows that as expected the BER is always less than this upper bound.
- The curves corresponding to upper bound given in Eqn. 3.17, Chernoff bound (Eqn. 3.14) and BER for  $m = 3$  are shown in Fig 5.7. It can be seen that the upper bound is looser than Chernoff bound. This could be the result of the fact that the upper bound on BER given by Eqn. 3.16 is derived from the maximum value of the integrand obtained over the interval of integration [13], whereas, Chernoff bound is derived from the density function.

## 5.1 Scope for Future work

This work has been carried out with the assumption that the number of paths and their delays do not change during call duration. It has also been assumed that delays are known to the receiver. In practical situations, number of paths and their delays keep on changing in accordance with the change in channel conditions. The work can be extended for practical situations by incorporating a timing acquisition circuit which adaptively estimates the number of paths and delays. Also the shape factor has been taken to be same for all the paths. Different values of  $m$  for different paths may provide a more realistic performance.

# References

- [1] Pickholtz, R. L., Schilling, D.L. and Milstein, L.B., "Theory of spread-spectrum communications - A Tutorial," *IEEE Transactions on Communications*, vol.COM-30,No.5, May 1982, pp. 855-883.
- [2] Viterbi, A. J., " Spread Spectrum Communications- Myths and Realities," *IEEE Communications Magazine*, Vol. 17, May 1979, pp. 11-18.
- [3] Viterbi A. J., " CDMA: Principles of spread spectrum communication," Addison-Wesley publishing,1995.
- [4] Dersch, U. and Ruegg, R. J., "Simulations of the Time and Frequency Selective Outdoor Mobile Radio Channel," *IEEE Transactions on Vehicular Technology*, Vol. 42, No. 3, August 1993, pp. 338-344.
- [5] Hirofumi Suzuki, "A Statistical Model for Urban Radio Propagation," *IEEE Transactions on Communications*, Vol. Com-25, No. 7, July 1977, pp. 673-680.
- [6] Minoru Nakagami, "The m-Distribution, a general formula for intensity distribution of rapid fading," in *Statistical Methods in Radio Wave Propagation*, W. G. Hoffman, Ed. Oxford, England: Pergamon, 1960, pp. 3-36.
- [7] Braun, W. and Dersch, U., "A physical mobile radio channel model," *IEEE Transactions on Vehicular Technology*, Vol. 40,No. 2, May 1991, pp. 472-482.
- [8] Price, R. and Green, P. E., "A communication technique for multipath channels," *Proc. IRE.*, March 1958, pp. 555-570.

- [9] Eng, T. and Milstein, L. B., "Coherent DS-CDMA Performance in Nakagami Multipath Fading," *IEEE Transactions on Communications*, vol.43, No. 2/3/4, Feb/Mar/Apr 1995, pp. 1134-1143.
- [10] Efthymoglou, G. P. and Aalo, V. A., "Performance Analysis of Coherent DS-CDMA Systems in a Nakagami Fading Channel with Arbitrary Parameters," *IEEE Transactions on Vehicular Technology*, Vol. 46, No. 2, May 1997, pp. 289-297.
- [11] Lee, J. S. and Miller, L. E., *CDMA Systems Engineering Hand Book*, Artech House, 1998.
- [12] Proakis, J. G. *Digital Communications*, 3<sup>rd</sup> Ed., NY, McGraw Hill, 1995.
- [13] Simon, M. K. and Alouini, M. S., *Digital communication over fading Channels*, John Wiley and Sons, INC. 2000.
- [14] Turin, G., Clapp, F. Johnston, T., Fine, S and Lavry, D., "A statistical model of urban multipath propagation," *IEEE Transactions on Vehicular Technology*, Vol. VT-212, No. 1, 1972, pp. 1-9.
- [15] Yip, Kun-Wah and Ng, Tung-Sang, "A Simulation Model for Nakagami-m Fading Channels,"  $m < 1$  " *IEEE Transactions on Communications*, vol.48, No. 2, Feb 2000, pp. 214-221.
- [16] Patzold, M., Killat, U., Laue, F., and Li, Y., " On the statistical properties of deterministic simulation models for mobile fading channels," *IEEE Transactions on Vehicular Technology*, vol.47, Feb. 1998, pp. 254-269.
-